ICRC 2001

The extended analysis of the Trek detector

B. A. Weaver and A. J. Westphal

Space Sciences Laboratory, University of California, Berkeley, CA 94720 7450, U.S.A.

Abstract. Extended-Trek is the continuation of the Trek ultraheavy cosmic-ray project. The Trek detector consisted of an array of stacks of 16 sheets of BP-1 track-etch glass. The detector was exposed on the *Mir* space station between 1991 and 1995. The first results of the Trek experiment were based on a maximum of 12 signal measurements for each cosmic-ray event. Extended-Trek increases this to a maximum of 32 measurements for a selected sample of cosmic-ray tracks. The selected sample comes from detector stacks which were calibrated with 10.6 A GeV Au at two zenith angles. The anticipated improvement in charge resolution allows a direct measurement of the abundance of Ir in the cosmic rays, the first odd-Z abundance in this range of charge.

1 Introduction

The Trek ultra-heavy cosmic-ray collector (Trek for short) was installed on the exterior of the *Mir* space station in 1991. The detector was composed of 150 stacks of sheets of BP-1 glass, a barium phosphate track-etch detector developed at the University of California at Berkeley (Wang *et al.*, 1988). The total surface area was about 1.2 m^2, and the effective aperture was about 1 sr. Each stack contained 16 sheets of 9 cm $\times$ 9 cm $\times$ 1.5 mm BP-1 glass. One third of Trek was returned to Earth in November 1993 in a dedicated re-entry capsule. The remainder was returned in November 1995 by Space Shuttle *Atlantis* (STS-74).

After recovery, all stacks were calibrated with 10.8 A GeV Au ions at the Alternating Gradient Synchrotron (AGS) at Brookhaven National Laboratory to correct for small variations in chemical composition. The first batch of glass returned was exposed to this beam at normal incidence, *i.e.*, with the beam directed exactly perpendicular to the stack of detectors. The remaining stacks were exposed to this beam at both 15° and 40° zenith angle, as measured with respect

Correspondence to: B. A. Weaver (weaver@curium.SSL-.Berkeley.EDU)

to the normal.

For Trek measurements in the platinum-lead region, we removed six sheets from each stack (numbers 1, 2, 7, 8, 13, and 14), allowing up to twelve measurements on a cosmic-ray track. The remaining sheets were reserved for later analysis. Further details of the etching and analysis may be found in the technical study of Weaver *et al.* (1998). The results in terms of cosmic-ray composition were reported by Westphal *et al.* (1998). These results were strongly inconsistent with the most widely-held model of cosmic-ray origin (Meyer, 1985; Webber, 1997).

2 Extended-Trek

2.1 New Techniques

After the first Trek analysis was completed, the remaining Trek glass was placed in cold storage. Since 16 sheets were available, up to 32 measurements of a single cosmic-ray track were possible. Crudely, one might expect an improvement of $\sim \sqrt{3}$ in the charge resolution if all these measurements were made. In addition, as demonstrated by Weaver *et al.* (1998), the uncertainty in the value of G measured by weight loss is a significant contribution to overall measurement dispersion. For the Extended Analysis of the Trek Detector (Extended-Trek for short), we have selected cosmic-ray tracks from the group of Trek stacks which were calibrated at two zenith angles. The two zenith angles allow a more precise measurement of G, the amount of material removed by etching, in addition to other consistency checks described by Weaver *et al.* (1998). We have etched the remaining ten sheets from each selected Trek stack and combined the measurements with the original Trek data set to obtain up to 32 measurements of each individual cosmic ray.

A novel feature of Extended-Trek is the coring technique. Instead of etching an entire sheet of glass we use a water-cooled diamond-tipped core drill to remove a 2.5 cm diameter wafer which is nominally centered on the cosmic-ray

track location. Thus the amount of glass to be etched is dramatically reduced. While the original Trek analysis required more than 20 etches, the Extended-Trek etching was completed with *only two* primary etches with no change in the etch tank. The cost of etchant is always significant, and, especially in the case of HF, disposal costs can more than double the final cost of a quantity of etchant.

The uniform size of Extended-Trek wafers allows us to maximize the amount of scanning which can be performed on our existing microscope stage. In the original Trek analysis, the size of the sheets limited the number of automated scans which could be performed in one session. Now we are limited by the physical range of motion of the stage, and can perform 49 automated calibration scans after a single setup.

In addition, we have made a number of advances in data analysis. The first advance is in the automated measurement of cosmic-ray signal. Each cosmic-ray etch-pit is electronically photographed and the image is passed through an image processor which produces a threshold gradient image. The pixels which make up the rim of the etch-pit are selected and their coordinates are written to a file. Occasionally, the cosmic-ray etch-pit will intersect small over-etched pits due to low-charge, low-energy cosmic rays. These can break up what would otherwise be an essentially perfect ellipse. In the past we have removed the pixels due to these defects by manually editing the file containing the pixel coordinates. However, we have found a technique for automatically editing these files, provided the defects are not too large. We start by fitting an ellipse to the unedited coordinates. We then identify the pixels which fall outside the fitted ellipse and which are farthest from the fitted ellipse. These pixels are removed from the analysis, and the fit is repeated on the remaining pixels. This process is repeated until all remaining pixels lie 1μm or less from the fitted ellipse. This technique has reduced the amount of manual editing required by roughly an order of magnitude.

Another advance has been made in the automated identification of orbital electron attachment. The short sampling distance and excellent charge resolution of BP-1 allow us to observe cases where a cosmic-ray nucleus has temporarily captured a single orbital electron. To automatically identify such events, we first perform a maximum-likelihood fit to the signal-versus-distance data with the assumption that the cosmic-ray charge remains constant throughout. Then for each pair of adjacent surfaces we reevaluate the likelihood holding the energy fixed and reducing the charge by one unit for only that pair of surfaces. If the χ^2 is reduced, we assume that an electron attachment has taken place. Finally we repeat the complete maximum-likelihood analysis with the identified charge offsets. Figure 1 shows an example of an electron attachment which was automatically identified in the analysis.

In a similar way we are also able to automatically identify "reverse" events. The Trek stacks were oriented with respect to *Mir* such that sheet 1 was furthest from the hull and sheet 16 the closest. A "forward" directed cosmic ray is one which entered the Trek stack passing through sheet 1 first and then proceeding deeper. A "reverse" event is one which entered the Trek stack starting on sheet 16, and incidentally passed through some of *Mir* before reaching the Trek detector. There are two ways to tell the direction of a cosmic ray. First, if the particle is of sufficiently low energy, as it loses energy in the detector, its value of detector response will increase. If x is the depth of the cosmic-ray track in the detector measured along the track and increasing from sheet 1 to sheet 16, then we estimate the rate of change in track-etch signal with respect to x. If this rate of change is sufficiently large and negative, we identify the particle as a reverse event. This does not work for high-energy cosmic rays for which the rate of change in signal is approximately zero. However, it is possible to determine direction for relativistic particles which undergo nuclear fragmentation in the detector. The probability of losing one or more charges is much greater than the probability of gaining a charge, and the probability of gaining more than one charge is essentially zero. Thus, if the charge of the particle appears to increase (discontinuously) with increasing x, this is most likely a "reverse" cosmic ray which has lost some charge due to nuclear fragmentation. If neither of these methods suggest a definite direction, we analyze the data in both directions and assign the direction which has the smaller χ^2. Approximately 25% of Extended-Trek events were identified as reverse events.

2.2 Analysis

In Figure 1 we show an example of a final Extended-Trek measurement. For each surface, we have measured the signal due to the cosmic ray and performed a calibration scan of the surrounding area. The cosmic-ray signal is corrected using the difference between the calibration signal and a standard value for Au at 10.8 A GeV. We also measure the zenith angle of the event and compute the flight distance of the cosmic ray. The signal-versus-distance data are all that are needed to perform a fit to determine the cosmic-ray charge and energy. The subsequent data analysis procedure was similar to that used in the original Trek analysis. This procedure is described in more detail by Weaver (2001).

2.3 Error Analysis

In much the same way as the original Trek analysis, we performed Monte Carlo simulations of the detector in the new configuration using measured values of dispersion in various parameters to generate dispersions in charge. The simulation was performed using measured charges and energies but with six times the statistics. Many of the sources of dispersion are the same as in the original Trek analysis. Though the magnitudes are mostly the same, the contribution to charge dispersion is reduced by the increased statistics.

We have identified two new contributions to dispersion, namely "missing" surfaces and "walk-offs." Missing surfaces are those surfaces which, for one reason or another, could not be included in the analysis. For example, a wafer may have shattered during coring, or the etch-pit of the cos-
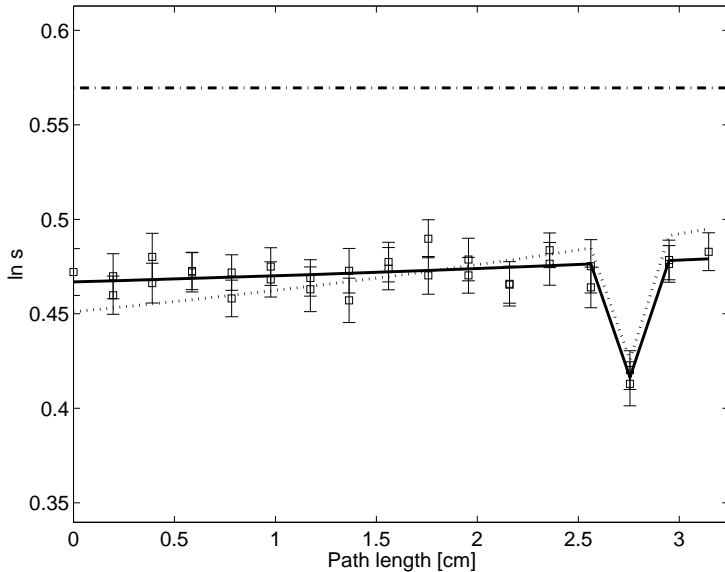
Fig. 1. Track-etch signal ($\ln s$) plotted versus flight distance in a Trek detector stack for a typical ultra-heavy cosmic ray. Individual measurements are indicated by the square points with error bars. The solid line indicates the expected values for the best-fit charge, Z, and energy. The lower dotted line shows the expected values with the charge fixed at $Z - 1$ and with the energy free to vary. The dot-dashed line indicates the values for relativistic Au (the calibration beam). The dip in signal toward the end of the track is due to the temporary attachment of a single orbital electron and was automatically identified during the data analysis.

mic ray was masked by some surface defect. The average number of analyzable surfaces is consistent with roughly 5% missing surfaces, not counting walk-offs. The walk-offs are events which fragmented completely in the detector or which passed off the edge of the detector. In other words, these are a special category of missing surfaces in which after some number of surfaces all subsequent surfaces are missing.

The effects of electron capture and nuclear fragmentation have been eliminated from consideration since we now have full coverage of the cosmic-ray track. These effects are extremely easy to identify and correct, and so should not make a significant contribution to charge dispersion.

Further details of the error analysis are given by Weaver (2001). The total dispersion in charge was determined by two methods. First, dispersions due to the individual effects were added in quadrature. Second, a simulation was run with all contributions to charge dispersion added. The two methods were consistent with each other and predicted a charge resolution of $0.35e$.

2.4 Results

The histogram of measured charges is shown in Figure 2. This includes all events passing the cuts $E > 900$ A MeV, $Q(\chi^2|\nu) > 0.001$, $Z > 71$, and $Z < 84$. The charge cuts removed only two outliers, which, at least in the case of the high charge event, was probably mis-identified due to poor statistics (the event was close to the edge of a stack and "walked off"). Altogether 121 out of 146 (83%) Extended-Trek events passed these cuts. For comparison we also show the charge histogram of original Trek analysis data in Figure 3 with the same cuts applied, and the same bin size. It should be readily apparent to the unaided eye that the charge resolution has improved in the Extended-Trek analysis. The peaks at Os and Pb are particularly diagnostic in this case.

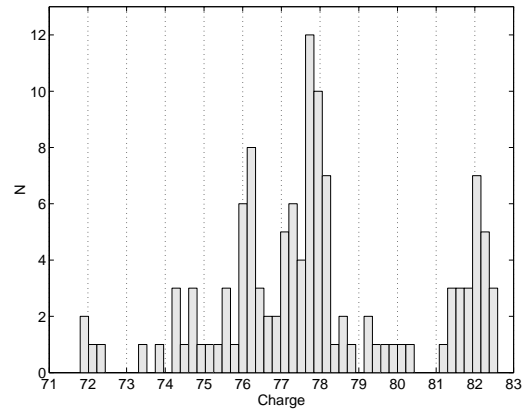To find the observed abundance the histogram in Figure 2

Fig. 2. Charge histogram for the Extended-Trek analysis.

was fitted to a set of Gaussians with peaks at integer charges between 72 and 83 and with resolutions between $0.3e$ and $0.4e$. The best fit to the observed data was with a charge resolution of $0.35e$, which is consistent with the resolution obtained from the Extended-Trek error analysis. The charge histogram with the fitted Gaussians is shown in Figure 4. The value of χ^2 reported in the figure is the value recommended for binned data with low statistics (Hikasa *et al.*, 1992), namely

$$\chi^2 = 2 \sum_k (y(x_k) - y_k) + y_k \ln\left(\frac{y_k}{y(x_k)}\right), \qquad (1)$$

where y_k is the number of events in the kth bin and $y(x_k)$ is the model prediction for that bin. When $y_k = 0$, the second term is zero.

To obtain the uncertainty in the fitted abundances, Monte Carlo distributions based on the fitted abundances were generated and fitted with the same procedure. The statistical un-
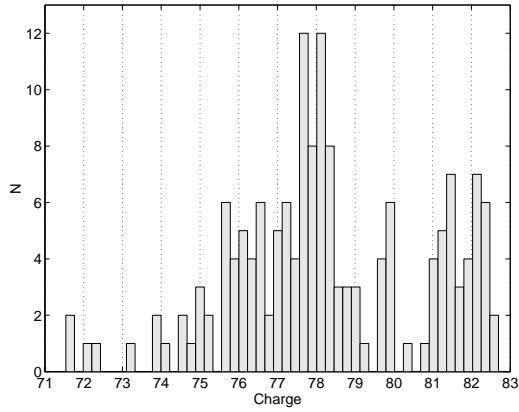
Fig. 3. Charge histogram for the original Trek analysis with the same cuts as applied to the Extended-Trek analysis.

Fig. 4. Charge histogram for the Extended-Trek analysis with fits to observed abundances.

certainty was determined from 63% lower and upper limits in the Monte Carlo simulation subtracted from the mean value of the abundances in the different resolution models. The systematic uncertainty was determined from the maximum and minimum abundances in the different resolution models subtracted from the mean values. The observed abundances are shown in Table 1.

Since the observed abundances are consistent with the original Trek analysis, the results (Westphal *et al.*, 1998) in terms of source abundances still stand. The abundance of Hg is slightly lower, but this does not significantly change the results of Westphal *et al.* (1998). The observation of a depletion of Ir relative to Os is confirmed. There is no way to find the source abundance of Ir since the propagation-corrected point-spread-function of Ir is strongly peaked at Pt, thus the point-spread-function of Pt will look very similar to that of Ir. This degeneracy leads to an intrinsic numerical instability in the derivation of source abundances.

3   Conclusion

It should now be clear that many of the advances needed for the analysis of next-generation track-etch detectors have al-

ready been achieved. The improvement in charge resolution has been demonstrated. We will probably be able to improve charge resolution even further in the next-generation detector, the Extremely Heavy Cosmic-Ray Composition Observer (ECCO). Since the detector modules planned for ECCO will be so large, the probability of walk-offs will be greatly reduced, although not entirely eliminated, since this category also includes events which fragment completely in the detector. This category could also be eliminated by only analyzing events which penetrate the detector completely.

References

Hikasa, K. *et al.*, Review of Particle Properties, *Phys. Rev. D*, **45**, 1, 1992.

Meyer, J.-P., Solar-Stellar Outer Atmospheres and Energetic Particles, and Galactic Cosmic Rays, *Astrophys. J. Supp.*, **57**, 173–204, 1985.

Wang, S. C., Barwick, S. W., Ifft, D., Price, P. B., Westphal, A. J., and Day, D. E., Phosphate Glass Detectors With High Sensitivity to Nuclear Particles, *Nucl. Inst. Meth. B*, **35**, 43–49, 1988.

Weaver, B. A., Westphal, A. J., Price, P. B., Afanasyev, V. G., and Akimov, V. V., Performance of the Ultraheavy Collector of the Trek Experiment, *Nucl. Inst. Meth. B*, **145**, 409–428, 1998.

Weaver, B. A., Actinides in the Cosmic Rays and Their Detection, Ph.D. Dissertation, University of California at Berkeley, 2001.

Webber, W. R., New Experimental Data and What It Tells Us About the Sources and Acceleration of Cosmic Rays, *Space Sci. Rev.*, **81**, 107–142, 1997.

Westphal, A. J., Price, P. B., Weaver, B. A., and Afanasyev, V. G., Evidence Against Stellar Chromospheric Origin of Galactic Cosmic Rays, *Nature*, **396**, 50–52, 1998.

Element	Observed Abundance
Hf	$0.073^{+0.028}_{-0.006}$ (stat.) $^{+0.002}_{-0.001}$ (syst.)
W	$0.061^{+0.014}_{-0.016}$ (stat.) $^{+0.003}_{-0.002}$ (syst.)
Os	$0.257^{+0.031}_{-0.031}$ (stat.) $^{+0.006}_{-0.007}$ (syst.)
Ir	$0.190^{+0.036}_{-0.038}$ (stat.) $^{+0.006}_{-0.009}$ (syst.)
Pt	$0.471^{+0.027}_{-0.036}$ (stat.) $^{+0.030}_{-0.031}$ (syst.)
Hg	$0.062^{+0.011}_{-0.014}$ (stat.) $^{+0.006}_{-0.003}$ (syst.)
Pb	$0.294^{+0.031}_{-0.028}$ (stat.) $^{+0.022}_{-0.023}$ (syst.)

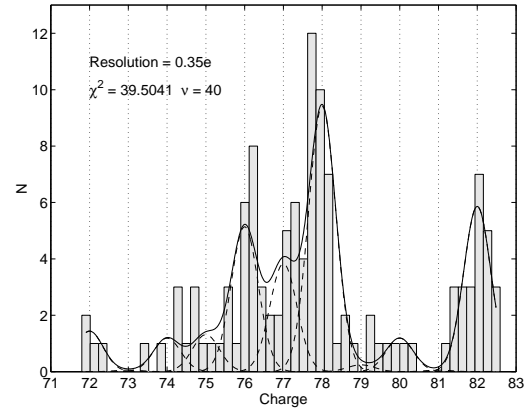**Table 1.** Observed abundances in the Extended-Trek analysis. All abundances are relative to the Pt-group: $75 \le Z \le 79$.